

## RECENT IMPROVEMENT OF THE APS BOOSTER SYNCHROTRON\*

C.-Y. Yao#, J. Wang, H.-R. Shang, S. Xu, R. Laird, V. Sajaev, N. Sereno  
Argonne National Laboratory, Argonne, IL 60439, USA

### Abstract

The APS booster injector is a 7-GeV electron synchrotron. Several improvements have been implemented in the booster area, including development of the 92-nm low emittance lattice, upgrade the ramp current readback ADCs, and development of a new firing card for the main ramp supplies. Recently we have completed commissioning of the low-emittance lattice and it is now the APS operational lattice. Combined with optimization of the storage ring lattice and injection, we have achieved close to 100% storage ring injection efficiency. This report presents the improvements and measured beam and performance of the ramp supplies.

### BOOSTER MAIN MAGNET CURRENT ADC UPGRADE

Recently we commissioned a new ADC module for the ramp supply current readback. The original module, a single ADC multiplexed 16-bit unipolar module, was obsolete and no longer supported. The new V490 module [1] is a 16-channel, 16-bit bipolar ADC VME module. Several hardware and software modifications were necessary to accommodate the new module including a synchronous external clock, a new DCCT bias and gain conversion card, and changes in both the IOC (iocbramp) and ramp correction programs. Figure 1 is a diagram of the ramp control system [2].

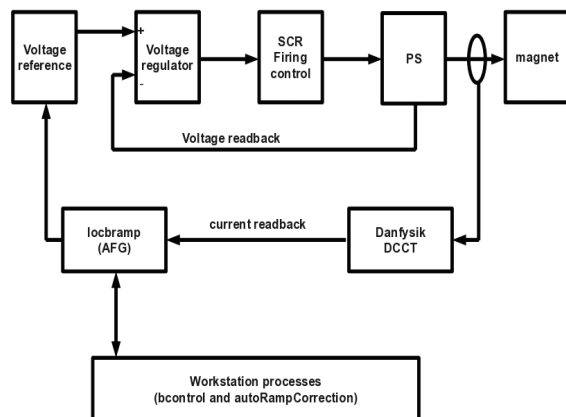


Figure 1: Block diagram of booster ramp control and correction system.

The power supplies implement voltage regulations. Voltage ramp waveforms are generated by arbitrary function generator (AFG) modules. The power supplies

\*Work supported by the U.S. Department of Energy, Office of Science, under Contract No. DE-ACO2-O6CH11357.

#cyao@aps.anl.gov

produce a regulated voltage output waveform to the magnets. Magnet current waveforms are monitored with DCCTs and acquired with ADC modules. Workstation-based ramp correction programs achieve current regulation through AFG amplitude and trigger delay adjustments and corrections to the AFG voltage reference ramps.

Figure 2 shows a block diagram of the hardware configuration for the new ADC acquisition system. The V490 module can read the magnet currents at an update rate of 2 Hz, four times faster than the old modules. In each ramp cycle there is only a time slot of 24 ms available for transferring all the data to VME memory. Considerable effort was spent to test and ensure the integrity of the data acquisition process. We also spent significant effort on adjusting ramp parameters to compensate for the real-time difference between the new and old ADC modules.

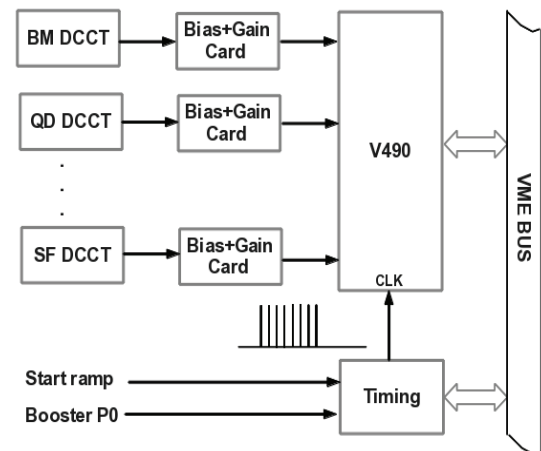


Figure 2: Configuration diagram of the new ramp current acquisition system.

After optimization of the parameters for ramp correction, the system works well. Measured data show a 30% improvement in  $dI/I$  rms error of the dipole and quads. We think the improvement is due to reduction of noise, more accurate sample timing of the new ADC module, and faster correction cycles. Figure 3 shows a plot of measured  $dI/I$  rms errors after the commissioning of the new ADC module. The improvement in ramp correction is also observed in booster transverse tune measurement. Tune variations, especially at injection time, is reduced from 0.01 to 0.006, as shown in Fig. 4.

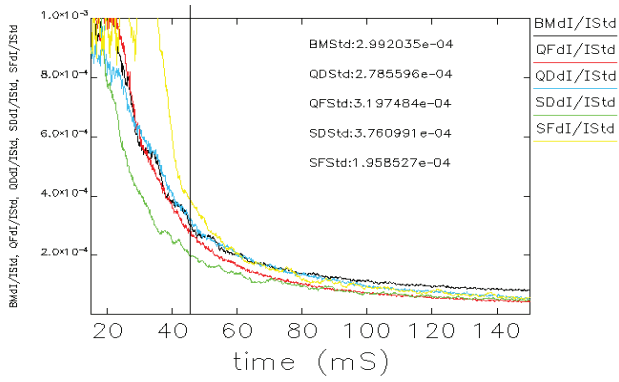


Figure 3: Measured booster ramp current  $dI/I$  standard deviation errors with the new ADC module. The vertical line marks injection time.

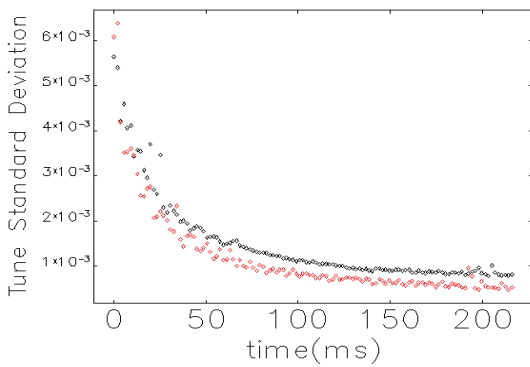


Figure 4: Measured shot-to-shot x- (black) and y-tune (red) standard Deviation of the 92-nm booster low-emittance lattice with the new ADC module.

### BOOSTER LOW-EMITTANCE LATTICE IMPROVEMENT

The booster 92-nm low-emittance lattice was successfully commissioned and has been installed as the operational lattice for user operation. Its main parameters are listed in Table 1.

Table 1: Main Parameters for the Booster 92-nm Lattice

Beam energy (GeV)	7
Max. Beta func. ( $\beta_x, \beta_y$ ) (m)	16.89, 22.20
Nominal tunes ( $\nu_x, \nu_y$ )	13.75, 5.80
Meas. tunes ( $\nu_x, \nu_y$ )	13.80, 5.65
Meas. Chromaticity ( $\xi_x, \xi_y$ )	1.0, 2.5 (inj) 4.0, 0 (ext)
Norm. emittance (nm)	92
Meas. emittance (nm)	69 **

\*\* Actual beam emittance is lower due to -0.4% off-momentum operations.

Tunes and chromaticity optimization played an important role in stabilizing shot-to-shot booster injection efficiency in the low-emittance booster lattice. We ran

*sddsoptimize* [3] to optimize the slope and start time of the current ramps of the two quad families for tune adjustment, and the two sextupole families for chromaticity adjustment. We were not able to adjust the tunes to the nominal values without losing injection efficiency. The final tunes after optimization are 13.80 and 5.65, in the x and y planes, respectively. Figure 5 and 6 show the measured final tunes and chromaticities.

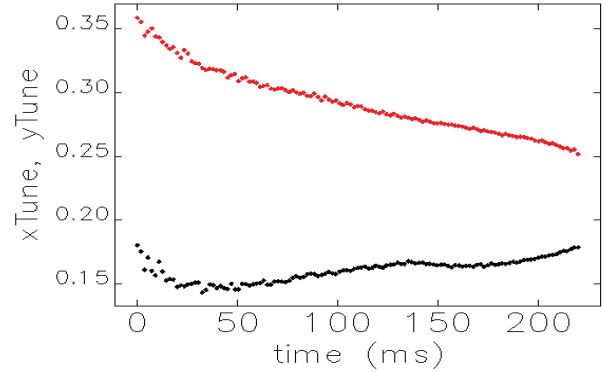


Figure 5: Measured x- (black) and y-tunes (red) of the booster 92-nm lattice. The tunes are detected at low sideband of revolution harmonic.

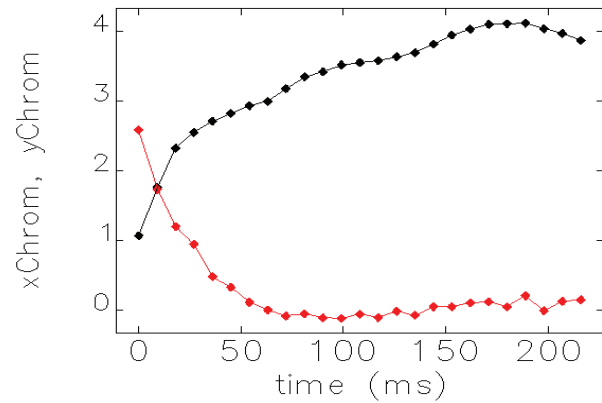


Figure 6: Measured x- (black) and y-chromaticity (red) of 92-nm booster lattice.

The booster has 40 horizontal and 39 vertical correctors. The ramp waveform generator of the corrector power supplies requires a 20-s update time, which makes orbit correction impractical. We implemented a 4-corrector-bump-scan application to optimize the booster orbit. The application divides the booster into 40 sectors and divides the corrector ramp into 3 time segments: at injection, at extraction, and in the middle of a ramp cycle. For each combination of plane, sector, and time segment, the application searches for the best orbit bump amplitude that maximizes injection efficiency. A current monitor waveform is used to monitor the effect of bump changes

and time of beam loss. A full scan can take many hours to complete. We found this application very effective for injection efficiency tuning.

The booster does not have skew quads for coupling corrections. We found that most of the coupling comes from vertical orbit drift during energy ramp. In order to minimize vertical orbit drift, we first set all the vertical corrector ramps to zero and then ran a vertical corrector bump scan with a minimal set of vertical correctors. This has reduced the number of non-zero correctors from 39 to a few and reduced the coupling by more than 50%.

## LATTICE MODELING WITH RESPONSE MATRIX FIT

In order to further confirm and characterize the low-emittance lattice, we measured the dispersion and orbit response, and ran a response matrix fit program with the data [4]. The fitting was good. Figure 7 shows the measured and the fitted  $\eta_x$  functions. Figure 8 shows fitted and design beta functions.

The booster quadrupole magnets are not powered individually. Therefore it is not possible to correct lattice functions. However, the result confirms that there are no major errors in the real machine lattice. The fit rms quads' strength k1 errors are around  $\sim 6 \times 10^{-3}$ . The difference between the fit beta functions and the designed values is around 6%.

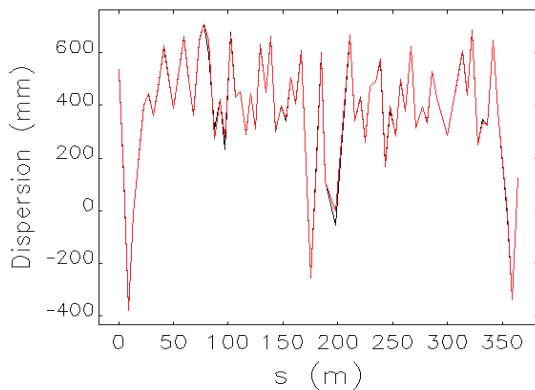


Figure 7: Measured (black) and model-fitted (red) x-dispersion of the booster low-emittance lattice.

## FUTURE IMPROVEMENTS

Several future upgrades are planned including: (1) development of a new sextupole supply that delivers higher strengths to the defocusing sextupoles; (2) non-linear ramp upgrade so we can correct tunes and chromaticities more effectively at injection; (3) installation of new firing cards on all main ramps supplies to provide better regulation resolution; (4) replacement of the corrector ramp controls to achieve a 2-Hz corrector ramp update rate, which is necessary to run orbit corrections.

## CONCLUSION

We successfully commissioned the booster ramp current new ADC module. The hardware and software implementation we adopted is effective and helped reduce programming and beam tuning efforts. The new module improved the stability of the ramp current with a measured dI/I rms error by 30%. Measured tune fluctuation also was reduced by 20%. Our efforts to optimize the low-emittance booster lattice achieved our goal of 100% booster injection efficiency, shot-to-shot beam stability, and design emittance. The lattice is installed for APS operations. We conclude that with a few additional moderate upgrades, the booster synchrotron can meet the needs of APS user operations and future upgrades.

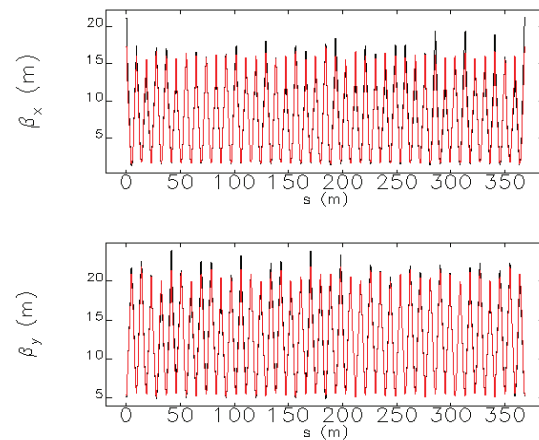


Figure 8: Measured and model  $\beta$ -functions of the booster low-emittance lattice. Black trace: fit result, red: design model.

## ACKNOWLEDGMENTS

We would like to thank Frank Lenkszus, Doug Horan, Nick DiMonte, Tony Puttkammer, Al Hillman, Karen Schroeder, Stan Pasky, Greg Fystro, and the APS operations crews for their assistance and support.

## REFERENCES

- [1] Highland Technology, "V490 16-channel VME multi-range digitizer," <http://www.highlandtechnology.com/DSS/V490DS.shtml>
- [2] CY Yao et al., "Upgrade of the APS Booster Synchrotron Magnet Ramp," PAC'11, TUP190, p. 1181 (2011).
- [3] L. Emery et al., "User's Guide for SDDS-compliant EPICS Toolkit Version 1.5," [http://www.aps.anl.gov/Accelerator\\_Systems\\_Division/Accelerator\\_Operations\\_Physics/manuals/EPICStoolkit/EPICStoolkit.html](http://www.aps.anl.gov/Accelerator_Systems_Division/Accelerator_Operations_Physics/manuals/EPICStoolkit/EPICStoolkit.html).
- [4] V. Sajaev, "Determination and Correction of the Linear Lattice of the APS Storage Ring," EPAC'02, TUPRI001, p. 742 (2002).